



**HAL**  
open science

## Blue mussels' valve behavior exhibits daily and lunar rhythms during the high Arctic polar day

Alexandre Le Moal, Laura Payton, Hector Andrade, Lionel Camus, Carl Ballantine, Pierre Ciret, Damien Tran

► **To cite this version:**

Alexandre Le Moal, Laura Payton, Hector Andrade, Lionel Camus, Carl Ballantine, et al.. Blue mussels' valve behavior exhibits daily and lunar rhythms during the high Arctic polar day. *Marine Biology*, 2023, 170 (9), pp.113. 10.1007/s00227-023-04257-6 . hal-04262345

**HAL Id: hal-04262345**

**<https://hal.science/hal-04262345>**

Submitted on 30 Oct 2023

**HAL** is a multi-disciplinary open access archive for the deposit and dissemination of scientific research documents, whether they are published or not. The documents may come from teaching and research institutions in France or abroad, or from public or private research centers.

L'archive ouverte pluridisciplinaire **HAL**, est destinée au dépôt et à la diffusion de documents scientifiques de niveau recherche, publiés ou non, émanant des établissements d'enseignement et de recherche français ou étrangers, des laboratoires publics ou privés.

1            **Blue mussels' valve behavior exhibits daily and lunar rhythms**  
2                            **during the high Arctic polar day**

3  
4 Alexandre Le Moal<sup>1</sup>, Laura Payton<sup>1, 2</sup>, Hector Andrade<sup>3</sup>, Lionel Camus<sup>4</sup>, Carl Ballantine<sup>4</sup>,  
5 Pierre Ciret<sup>1, 2</sup>, Damien Tran<sup>1, 2\*</sup>

6  
7 <sup>1</sup>University of Bordeaux, EPOC, UMR 5805, F-33120 Arcachon, France

8 <sup>2</sup>CNRS, EPOC, UMR 5805, F-33120 Arcachon, France

9 <sup>3</sup>Institute of Marine Research, 9007 Tromsø, Norway

10 <sup>4</sup>Akvaplan-niva, Fram Centre for Climate and the Environment, 9296 Tromsø, Norway

11  
12    **Corresponding author**

13    Damien Tran

14    E-mail : damien.tran@u-bordeaux.fr

15    **Keywords**

16    High Arctic, polar day, mussel, behavior, daily rhythm, lunar rhythm, semi-lunar rhythm, tidal  
17    rhythm.

18 **Abstract**

19 Marine species exhibit a multitude of biological rhythms, in accordance with their complex  
20 ecosystem governed by sun, earth and moon trajectories. Because of the inclination of the  
21 earth's axis, the high Arctic ecosystem is characterized by several months of permanent  
22 illumination during the polar day. The persistence of biological rhythms in this photic context  
23 remains unclear. Yet, this information is crucial for the understanding of polar ecosystems  
24 functioning, as well as to predict the impact of future climate changes. Particularly, the impact  
25 of extreme photoperiods on recent invasive species remains largely unknown. Here, we  
26 investigate how environmental cycles shape the behavior of a re-emerging polar resident, the  
27 mussel *Mytilus sp.* during polar day (17 April to 26 August 2020; Svalbard, Ny-Ålesund, 78°56'  
28 N, 11°56' E). Our results show that in the high Arctic polar day, mussels' behavior is shaped  
29 by both the photoperiod and the diel sun trajectories above the horizon. Additionally, mussels  
30 also exhibit tidal, semi-lunar, and lunar rhythms of valve opening amplitude. We argue that  
31 these rhythms may have ecosystems functioning implications, and that the mussels' ability to  
32 deal with drastic light regimes may explain their northward expansion and new resettlement in  
33 high Arctic.

34

## 35 **Introduction**

36 The high Arctic is undergoing major changes, including a fast decline in ice cover and  
37 warming at a rate that is two to four times faster than that the rest of the planet (2021; Chylek  
38 *et al.* 2022). These drastic changes are likely to have numerous ecological consequences, such  
39 as species poleward expansion, shift in trophic interactions, and reorganization of biological  
40 communities (Post *et al.* 2018; Beaugrand *et al.* 2019). In order to understand how the Arctic  
41 and its ecosystems are changing, focus needs to be directed toward a more factual  
42 understanding of today's biology in polar areas (Schmal *et al.* 2020).

43 Living organisms have evolved in complex biotopes governed by environmental cycles  
44 related to astronomical trajectories and interactions (Tessmar- Raible *et al.* 2011). The  
45 temporal coordination of biological processes with these cycles is crucial, from molecular to  
46 behavioral activities (Mermet *et al.* 2017; Helm *et al.* 2017). Endogenous clocks allow  
47 organisms to anticipate changes in their environment by using the highly predictable cycles as  
48 zeitgebers, such as the light / dark cycle. Due to the axis of rotation of the earth, the light /  
49 dark alternation disappears at polar latitudes during polar day and polar night, characterized  
50 by several months of permanent illumination and darkness respectively. Thus, the interest of  
51 the persistence of daily rhythms in polar ecosystems is questionable (Schmal *et al.* 2020).

52 Biological clocks are highly adaptive, but robust behavioral rhythms could be a drawback for  
53 adaptation to constant photic environments (Bloch *et al.* 2013; Abhilash *et al.* 2017; Bertolini  
54 *et al.* 2019; Schmal *et al.* 2020). The issue of the maintenance of biological rhythms during  
55 the polar day remains crucial for the understanding of polar ecosystems functioning, but also  
56 to predict the impact of future changes (Schmal *et al.* 2020; Huffeldt 2020; Hüppe *et al.* 2020;  
57 Perrigault *et al.* 2020; Payton *et al.* 2021). Indeed, the northward expansion of organisms  
58 originally located at more southern latitudes implies substantial daily changes in photic  
59 conditions. The impact of extreme photoperiods on invasive species remains unknown.

60 The blue mussel *Mytilus sp.* is recently resettled in the high Arctic after a 1000-year absence  
61 (Berge *et al.* 2005). It succeeded in Svalbard archipelago as a hybrid species, resulting from  
62 the mix of three species: *Mytilus edulis*, *Mytilus Galloprovincialis*, and *Mytilus trossulus*  
63 (Mathiesen *et al.* 2017; Leopold *et al.* 2019). The blue mussel is frequently used as an  
64 environmental indicator, as it is a semi-sessile organism, widely distributed in coastal regions  
65 in both hemispheres, with a relatively long-life span. As it has the potential to dominate  
66 benthic habitats in intertidal and shallow subtidal areas, the blue mussel plays an important  
67 ecological role as an ecosystem engineer, and also a commercial role in the shellfish industry

68 (Leopold *et al.* 2019). However, close to their northern limit of distribution, *Mytilus* rarely  
69 occur in the intertidal areas because of cold winter aerial temperatures, but rather occur in  
70 subtidal areas at depths down to approximately 5 m (Mathiesen *et al.* 2017). The blue mussel  
71 possesses a functional endogenous circadian clock machinery (Chapman *et al.* 2017, 2020).  
72 As a bivalve organism, it shows valve opening behavioral rhythms, closely related to  
73 physiological processes such as breathing and nutrition, synchronized by environmental  
74 factors (García-March *et al.* 2008; Tran *et al.* 2011). A recent study has shown that both  
75 moonlight and sunlight oscillations below the horizon shape the blue mussel's valve behavior  
76 during the high Arctic polar night (Tran *et al.* 2023). However, how do mussels control their  
77 valve behavior during the high Arctic polar day remains unknown.  
78 The objective of this work was to better understand the ability of *Mytilus sp.* to maintain, or  
79 not, functional biological rhythms in polar regions, with a focus on polar day period when the  
80 sun is permanently above the horizon. First, we investigated the pattern of valve behavior  
81 according to seasons and then focusing on polar day. Then, we investigated the existence of a  
82 valve behavior daily rhythm, as well as the presence of tidal, semilunar, and lunar rhythms of  
83 *Mytilus sp.* during polar day. The results of this study provide key knowledge on the  
84 adaptation of temperate species that currently colonize polar environments.

85

## 86 **Material and methods**

### 87 **Animals, study area and data collection**

88 This study analyzes valve behavior data of 15 *Mytilus sp.* mussels ( $67.1 \pm 2.7$  mm shell  
89 length) recorded over a 15-month period (from 01/09/2019 to 27/11/2020), with a focus on  
90 polar day, from 17 April to 26 August 2020 (132 days). The study was conducted in  
91 accordance with local legislation. The mussels were collected manually by a diver from  
92 natural recruitment in the Isfjorden, near Longyearbyen (latitude  $78^{\circ}13'N$ , longitude  
93  $15^{\circ}38'E$ ), Svalbard. They were equipped with electrodes to record their behavior at 10 Hz  
94 using a high-frequency non-invasive (HFNI) valvometer biosensor (Payton *et al.* 2017a).  
95 Mussels were placed at the seafloor, always in subtidal conditions, at a depth of 3 m ( $\pm$  tides)  
96 in a ballasted cage (50 x 50 x 100 cm) under an old pier in Kongsfjorden near Ny-Ålesund  
97 (western coast of Spitsbergen Island, Svalbard;  $78^{\circ}56' N$ ,  $11^{\circ}56' E$ ) the 01/09/2019 (Fig. 1a).

98

### 99 **Environmental data acquisition**

100 Water temperature was measured every 10 sec, near the mussels, by our HFNI valvometer  
101 biosensor using a temperature sensor (ADT7420 sensor, Analog Devices). The astronomical  
102 data related to sun, earth, and moon positions during polar day were retrieved from the site  
103 <https://www.timeanddate.com> for the lunar cycles and <https://planetcalc.com> for the sun angle  
104 elevation. Tidal data measured in Ny-Ålesund (78°55' N, 11°56' E) were obtained from  
105 <https://www.kartverket.no>. Astronomical positions and environmental parameters are  
106 available in Supplementary Information S1. The map of the study area (Fig. 1a) was created  
107 in RStudio (R Core Team 2013) using the package ggOceanMaps (Vihtakari 2022). All times  
108 are expressed in UTC.

109

## 110 **Valve behavior**

### 111 **Principle of measure to record mussel valve activity**

112 Two lightweight electrode sensors designed to minimize disturbance to mussel behavior were  
113 glued on both shells (Tran *et al.* 2003; Andrade *et al.* 2016). These sensors were connected to  
114 the valvometer biosensor by flexible wires, which allowed the mussels to move their shells  
115 without constraints. The measurement is magnetic principle based. The sensors are made with  
116 small self-inductance coils (material: ferrite; size: 3.2 mm x 2.5 mm x 2 mm; weight: ~0.06  
117 g), whose specifications are: inductance: 470  $\mu$ H; rated current: 45 mA; self-resonance  
118 frequency: 5 mHz. Thanks to these sensor specificities, a very low electromagnetic field (~1-  
119 2 nT) was generated between the electrodes by the biosensor, allowing to measure valve  
120 opening amplitude. The signal was recorded at 10 Hz using custom acquisition cards (Nanog  
121 manufacturer, Pessac, France), and the data were automatically transmitted daily to a data  
122 processing center at the Arcachon Marine Station (France) using internet network (54 000  
123 data / day / mussel).

### 124 **Valve behavior quantification**

125 Field valve activity data were analyzed using LabView 8.0 software (National Instruments).  
126 The valve behavior endpoints were expressed as the hourly valve opening amplitude (VOA,  
127 %) of each individual (individual hourly valve opening amplitude data during polar day 2020  
128 are available in Supplementary Information S2). The hourly VOA was reported as a  
129 percentage, with 100 % indicating that the valves were opened at their maximum amplitude  
130 during the entire hour, and 0 % indicating that the valves were closed during the entire hour.  
131 All times are expressed in UTC.

132

## 133 **Temporal data set**

### 134 **Seasonal time cutting**

135 The mean valve opening amplitude (VOA, %) of 15 *Mytilus sp.* was calculated for each polar  
136 season (here, the use of “season” term is not in its classical acceptation, but adapted to polar  
137 environment) (Fig. 1b): period of diel light dark alternation around autumn equinox (from  
138 01/10/2019 to 24/10/2019 and from 26/08/2020 to 24/10/2020), polar night (when the sun is  
139 permanently below the horizon, from 25/10/2019 to 17/02/2020 and from 25/10/2020 to  
140 27/11/2020), period of diel light dark alternation around spring equinox (from 18/02/2020 to  
141 16/04/2020), and polar day (when the sun is permanently above the horizon, from 17/04/2020  
142 to 26/08/2020). Resulting data are available in Supplementary Information S3.

### 143 **Polar day investigation**

144 The investigation of mussels’ behaviour focused on the polar day, when the sun was  
145 permanently above the horizon, from 17 April 2020 to 26 August 2020 (132 days), meaning a  
146 dataset of 3 168 hourly VOA data per individual (n = 15 mussels, i.e. 47 520 data in total,  
147 available in Supplementary Information S2). From hourly VOA, daily VOA were calculated (n  
148 = 15 mussels, i.e. 1 980 data).

### 149 **Time cutting of the polar day**

150 To go deeper in the investigation, the polar day was -divided into 8 parts of 14-16 days, each  
151 part corresponding to a neap-spring tidal cycle (Supplementary Information S1).

### 152 **Different phases of significant biological rhythms tested**

153 When a significant daily, tidal, semi-lunar or lunar rhythm was identified (see  
154 “Chronobiological analysis” below), the VOA oscillations during the corresponding  
155 geophysical cycles were identified. For individuals with a significant daily rhythm, mean VOA  
156 was calculated individually at 4 phases (6 h ranges per phase) of daily cycles (n = 132 cycles):  
157 midnight (21h-3h), AM (3h-9h), midday (9h-15h) and PM (15h-21h). For individuals with a  
158 significant tidal rhythm, mean VOA was calculated individually at 4 phases (3h ranges per  
159 phase) of tidal cycles (n = 255 cycles): ebb tide, flow tide, high tide, and low tide  
160 (Supplementary Information S1). For individuals with a significant semi-lunar rhythm, mean  
161 VOA was calculated individually according to 4 tidal coefficient categories: highest,  
162 intermediate / decreasing, lowest, and intermediate / increasing tidal coefficients  
163 (Supplementary Information S1). In individuals with a significant lunar rhythm, mean VOA  
164 was calculated individually at 4 phases (7-9 days ranges per phase) of synodic lunar cycles (n  
165 = 4 cycles): new moon, first quarter of the moon, full moon and third quarter of the moon

166 (Supplementary Information S1). All times are expressed in UTC. Resulting data are available  
167 in Supplementary Information S3.

168

## 169 **Statistical analyses**

### 170 **VOA differences between season**

171 VOA differences between season were tested on mean seasonal individual VOA values  
172 (Supplementary Information S3). Significant differences between the rhythms' phases were  
173 tested using ANOVA on ranks (because of the non-normality of the data) for repeated measures  
174 (Friedman Repeated Measures Analysis of Variance on Ranks), followed by Student-Newman-  
175 Keuls method, using Sigma Plot software (Version 13.0; Systat Software, USA).

### 176 **Random components mixed model for repeated measures**

177 A random components mixed model for repeated measures was applied, knowing that the VOA  
178 data were not independent, to test the effects and the interactions of the maximum sun elevation  
179 angle (around midday), the water temperature, the direction of sun elevation (i.e. increasing sun  
180 max. elevation from the beginning of polar day to the summer solstice; or decreasing sun max.  
181 elevation from summer solstice to the end of the polar day) and the lunar phases (new moon /  
182 1<sup>st</sup> quarter moon / full moon / 3<sup>rd</sup> quarter moon) on individual daily VOA values, using XLSTAT  
183 2022 software (Addinsoft. New York, USA).

### 184 **VOA differences between phases of significant biological rhythms**

185 When a significant daily, tidal, semi-lunar or lunar rhythm was identified (see  
186 "Chronobiological analysis" below), VOA differences between the corresponding phases were  
187 tested on mean individual VOA values, only in mussels with a significant rhythm  
188 (Supplementary Information S3). Significant differences between the rhythms' phases were  
189 tested using ANOVA on ranks (because of the non-normality of the data) for repeated measures  
190 (Friedman Repeated Measures Analysis of Variance on Ranks), followed by Student-Newman-  
191 Keuls method, using Sigma Plot software (Version 13.0; Systat Software, USA).

192

## 193 **Chronobiological analysis**

194 In order to determine the existence of biological rhythms in mussel's behavior,  
195 chronobiological analysis were done on individual hourly VOA data, either on the whole polar  
196 day period, or on each of the 8 neap-spring tidal cycles of the polar day. Results are summarized  
197 in Supplementary Information S4.



**Determination of tested periods**

Four biological rhythms were investigated: daily rhythm, tidal rhythm, semi-lunar rhythm, and lunar rhythm. The corresponding geophysical cycles susceptible to synchronize these biological rhythms were (respectively): daily cycle (24h), tidal cycle (12.4h), neap-spring tidal cycles (14.7 d), and synodic moon cycle (29.5 d). Thus, rhythms were searched in the period ranges of:  $24 \pm 4$  h for daily rhythm,  $12.4 \pm 2$  h for tidal rhythm,  $14.7 \pm 2.5$  d for semi-lunar rhythm, and  $29.5 \pm 5$  d for lunar rhythm.

**Determination of significant rhythms**

Chronobiological analyses were performed using TSA Serial Cosinor 8.0 software. Several steps were required to validate a significant rhythm (Gouthiere *et al.* 2005; Tran *et al.* 2011). Four steps must be validated. First, the quality of the data set was assessed by controlling for the absence of randomness using the autocorrelation diagram (Box *et al.* 2015). Second, the absence of a stationary phenomenon was checked by using a partial autocorrelation function (PACF) calculation (Box *et al.* 2015). Third, the recorded data were tested for periodicities by the spectral method of the Lomb and Scargle periodogram, which combines the principle of a regression analysis and Fourier transformations (Scargle 1982). This method gives a threshold of probability ( $p = 0.95$ ) defining the limit below which the signal can be regarded as “noise”. Fourth, the rhythmicity was validated and modeled with the Cosinor model, which uses a cosine function calculated by regression (Nelson *et al.* 1979; Bingham *et al.* 1982). For a given period, the model is written as  $Y(t) = A \cos(\pi t/\tau + \phi) + M + \varepsilon(t)$  where  $Y(t)$  is an observation of the mean VOA at time  $t$ ,  $A$  is the amplitude,  $\phi$  is the acrophase,  $\tau$  is the period,  $M$  is the mesor and  $\varepsilon$  is the relative error. Two key tests validated the calculated model and the existence of a rhythm: the elliptic test had to be rejected, and the probability for the null amplitude hypothesis had to be  $< 0.05$ . For a set of data, several significant periodicities could occur. To identify significant secondary periodicities, we reinjected the previously calculated residues of the Cosinor model to remove the trend related to the first statistical period and then repeated the entire procedure (1-4 steps). This entire procedure was necessary to validate secondary periodicities. In this study, the procedure was repeated up to four times to reveal significant rhythmicity in the range of the studied rhythms.

227

228 **Results**

229 **Seasonal behavior**

230 In high Arctic conditions, in Ny-Ålesund, Svalbard (Fig. 1a), the mean valve opening  
 231 amplitude (VOA, %) of 15 *Mytilus sp.* was significantly higher during polar day;  $74.9 \pm 0.7$   
 232 %, mean  $\pm$  SE) than during the other periods of the year including the polar night ( $38.8 \pm 1.3$   
 233 %), and the two periods with diel alternation of light and dark centered either on the autumnal  
 234 equinox ( $65.3 \pm 1.5$  %) or on the spring equinox ( $30.8 \pm 1.6$  %) (Fig. 1b).

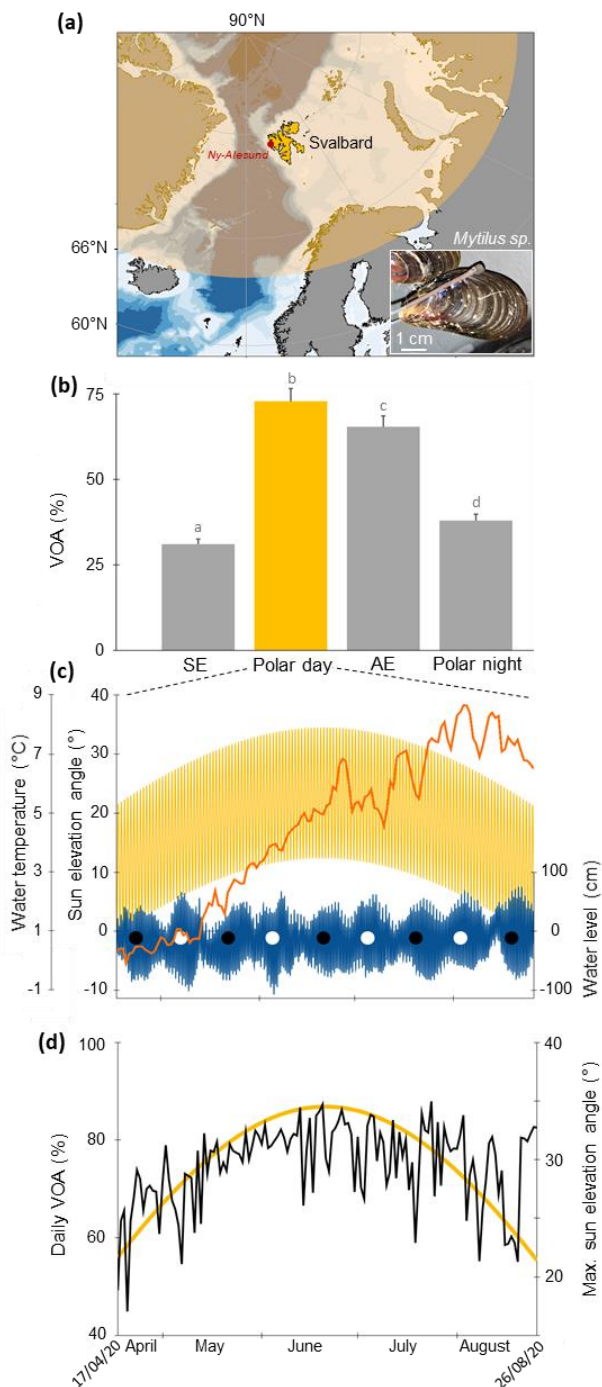


**Fig. 1 Context of the study, physical parameters, and mussels valve behavior during polar day.** (a) Ny-Ålesund location ( $78^{\circ}56' N$ ,  $11^{\circ}56' E$ ) and limit of polar day extension (yellow color surface). Insert with one of the 15 *Mytilus sp.* equipped with HFNI valvometer electrodes. (b) Mean hourly valve opening amplitude (VOA, %; mean  $\pm$  SE;  $n = 15$ ) during polar day (yellow bar) and other periods of the year, including light / dark alternation periods centered on Spring Equinox (SE) and Autumn Equinox (AE), and polar night. Different letters indicate significant differences ( $p < 0.05$ ). (c) Profiles of physical parameters of the studied site during polar day 2020: hourly sun elevation angle above the horizon (yellow); hourly sea water level (blue) and lunar phases (new moon: black circle; full moon: white circle); daily water temperature (orange). (d) Mean daily VOA (%;  $n=15$ ) during polar day with the daily maximum sun elevation angle above the horizon in yellow (see Supplementary information S5 for individual variability).

### 235 **Astronomical positions and environmental parameters during the polar day**

236 The studied polar day comprised 132 days, 255 tidal cycles, 8 neap-spring tidal cycles, and 4  
 237 entire synodic lunar cycles (Fig. 1c; Supplementary Information S1). At the location site, the  
 238 sun remained permanently above the horizon but still showed diel altitude cycles (24 h) with a  
 239 constant delta of 22.2° between daily min and max sun elevation. The diel maximum sun  
 240 elevation angle (around midday) increased during polar day and reached a maximum at  
 241 summer solstice (21/06/2020, 34.5°) before decreasing during the second part of polar day .  
 242 Ny-Ålesund site exhibited semi-diurnal tidal cycles (12.4 h) of ± 30 cm to ± 80 cm depending  
 243 on neap-spring tidal cycle (14.7 d). Neap-spring tidal cycles are cycles of tidal amplitudes that  
 244 occur two times per synodic lunar month cycles (29.5 d). Finally, water temperature recorded  
 245 near the mussels showed a regular increase during polar day.

### 246 **Behavior during polar day**

247 Fig. 1d showed that the mean daily valve opening amplitude (VOA) during polar day tended  
 248 to follow the course of the sun elevation in the sky (individual daily VOA were plotted in  
 249 Supplementary Information S5). In Table 1, individual daily VOA dataset was used. The  
 250 mixed model showed a significant random effect for “days” and “mussels” individual  
 251 parameters. Significant effects on VOA of the fixed parameters “daily sun maximum  
 252 elevation” and “lunar phases” were shown. No significant effects of “water temperature” or  
 253 “sun direction” parameters were shown. Finally, there was a significant effect of the  
 254 interaction between “sun maximum elevation” and “lunar phases” parameters on VOA.

255

256 **Table 1** Random components mixed model for repeated measures applied to test the effects of  
 257 daily sun maximum elevation, water temperature, sun direction (i.e. increasing (before summer  
 258 solstice) or decreasing (after summer solstice) sun max. elevation) and lunar phases on  
 259 individual daily VOA. Asterisks indicate significant *p*-value.

#### **Random components mixed model for repeated measures**

Covariance parameters	Z	<i>p</i> -value	
Random effects			
Days	6.470		< 0.0001***
Individuals	2.434		0.007**
Repeated factors	29.815		< 0.0001***
Source of variation (fixed parameters)	NumDF	F	<i>p</i> -value
Quantitative parameters			
Daily sun max. elevation	1	5.987	0.016*

Water temperature	1	2.007	0.159
Qualitative parameters			
Sun direction	1	1.085	0.299
Lunar phases	3	2.809	0.042*
<b>Interactions</b>			
Daily sun max. elevation x Temp.	1	1.912	0.169
Daily sun max. elevation x Sun direction	1	1.016	0.315
Daily sun max. elevation x Lunar phases	3	2.784	0.044*
Sun direction x Temperature	1	0.434	0.511
Sun direction x Lunar phases	3	0.035	0.991
Lunar phase x Temperature	3	0.573	0.634

260 \*  $p < 0.05$ , \*\*  $p < 0.01$ , \*\*\*  $p < 0.001$ .  
 261

## 262 Behavioral rhythms during polar day

### 263 Daily rhythm

264 Based on the hourly dataset, individuals chronobiological analyzes showed a significant daily  
 265 VOA rhythm for 93.3 % of mussels, with a mean period length of  $24.13 \pm 1.06$  h (Fig. 2a). In  
 266 rhythmic individuals, the VOA was the highest around midday and the lowest around  
 267 midnight, while intermediate at morning and afternoon (Fig. 2b). To investigate if the daily  
 268 rhythm evolved along polar day, the 132 days were divided in 8 neap-spring tidal cycles, and  
 269 new chronobiological analyzes were performed on each of these parts (Fig. 2c). No trends  
 270 appeared, neither in the percentage of rhythmic individual nor in the period lengths of daily  
 271 rhythms.

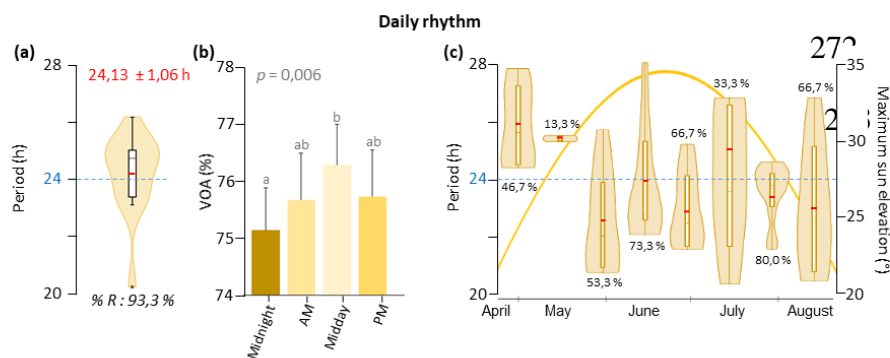
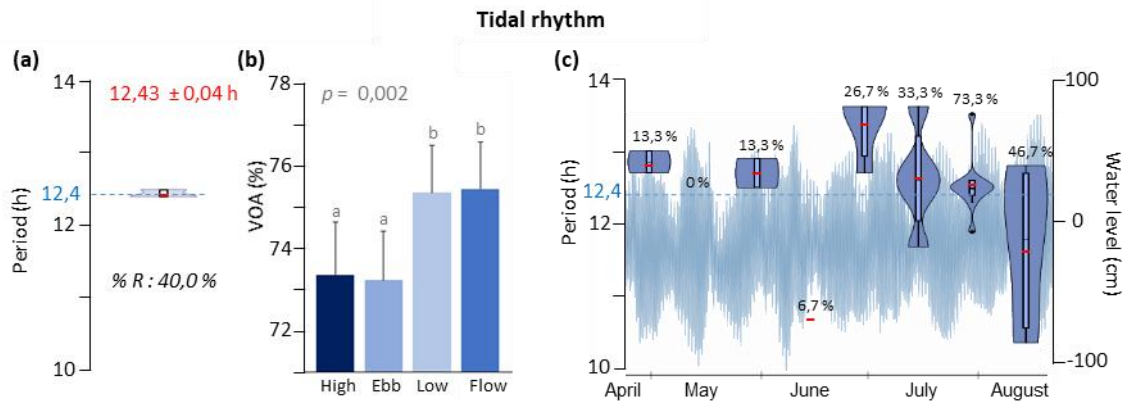


**Fig. 2 Chronobiological analysis: daily rhythm of mussels VOA behavior during polar day.**

(a) Individual significant circadian period lengths distribution is shown as a violin plot. The mean ( $\pm$  SE) period length is indicated in red. “% R” indicates the percentage of rhythmic mussels. The period length of the corresponding geophysical cycle is indicated in blue. (b) Mean VOA according to daily phases in rhythmic individuals. (c) Daily rhythm progression along polar day ( $n = 8$  parts / polar day), with the daily maximum sun elevation angle in yellow. Identical letters indicate no significant differences ( $p$ -value = 0.05).

274 **Tidal rhythm**

275 40 % of mussels exhibited a tidal rhythm, with a mean period length of  $12.43 \pm 0.04$  h (Fig.  
 276 3a). For these mussels, VOA was the lowest at high and ebb tides, and the highest at low and  
 277 flow tides (Fig. 3b). No trends of tidal rhythm's modulation along polar day appeared (Fig.  
 278 3c).



279

**Fig. 3 Chronobiological analysis: tidal rhythm of mussels VOA behavior during polar day.**

(a) Individual significant tidal period lengths distribution is shown as a violin plot. The mean ( $\pm$  SE) period length is indicated in red. “% R” indicates the percentage of rhythmic mussels. The period length of the corresponding geophysical cycle is indicated in blue. (b) Mean VOA according to tidal phases in rhythmic individuals. (c) Tidal rhythm progression along polar day (8 parts / polar day) and hourly tidal water level (blue). Identical letters indicate no significant differences ( $p$ -value = 0.05).

280

281 **Semilunar and lunar rhythms**

282 86.7 % of mussels showed a significant semilunar rhythm, with a mean period length of  $14.90$   
 283  $\pm 0.41$  d (Fig. 4a). The highest VOA were observed at low, decreasing, and high tidal  
 284 coefficients, while the lowest VOA were observed at increasing tidal coefficients (Fig. 4b).  
 285 Finally, 73.3 % of mussels showed a significant lunar rhythm, with a mean period length of  
 286  $29.22 \pm 0.39$  d (Fig. 4c). The mean VOA was the highest at first quarter moon and decreased

287 gradually at full moon before reaching a minimum at third quarter moon and new moon (Fig.  
 288 4d).

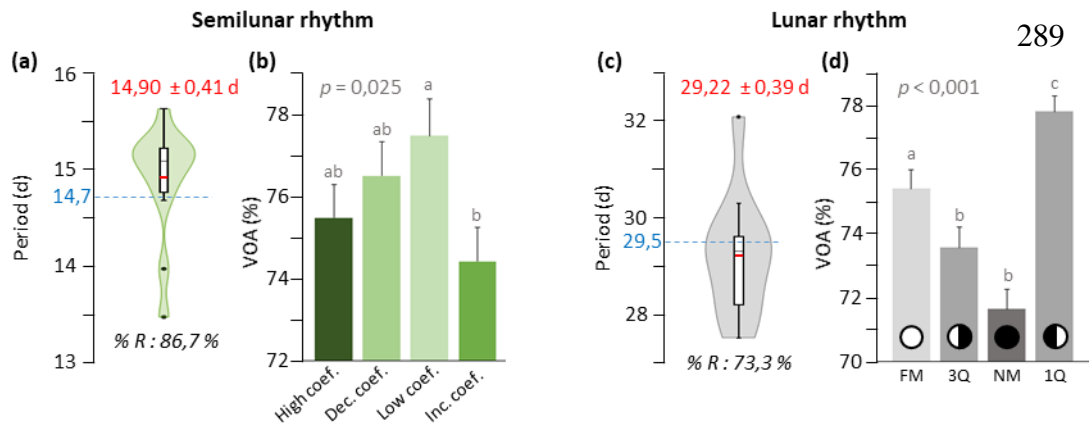


**Fig. 4 Chronobiological analysis: semilunar and lunar rhythms of mussels VOA behavior during polar day**

(a, c) Individual significant semilunar (a) and lunar (c) period lengths distribution are shown as violin plots. The mean ( $\pm$  SE) period length are indicated in red. “% R” indicate the percentage of rhythmic mussels. The period lengths of the corresponding geophysical cycle are indicated in blue. (b) Mean VOA according to tidal coefficients in individuals with a significant semilunar rhythm. (d) Mean VOA according to lunar rhythm phases in individuals with a significant semilunar rhythm. Identical letters indicate no significant differences ( $p$ -value = 0.05).

290 **Discussion**

291 Our findings clearly show that although the sun remains permanently above the horizon, the  
 292 re-emerging polar resident *Mytilus sp.* exhibit multitude behavioral rhythm periodicities  
 293 during the high Arctic polar day. First, behavioral valve activity of *Mytilus sp.* follows the sun  
 294 seasonal trajectory in the sky during polar day. Second, mussels exhibit a daily rhythmic  
 295 component in their behavior. Finally, mussels also show valve activity rhythms related to the  
 296 tidal, semi-lunar and lunar cycles.

297  
 298 The marine ecosystem is governed by a multitude of environmental cycles linked to the  
 299 celestial movements and interactions of earth, moon and sun. These environmental cycles  
 300 shape the biology of marine species, that exhibit a variety of biological rhythms already  
 301 widely documented (Häfker and Tessmar-Raible 2020; Andreatta and Tessmar-Raible 2020;  
 302 Kaiser and Neumann), from daily and tidal rhythms, to semi-lunar, lunar and seasonal  
 303 rhythms. Corresponding endogenous clock(s), synchronized by the corresponding predictable  
 304 and reliable abiotic cues, exist for most of these biological rhythms (Tessmar- Raible et al.  
 305 2011; Häfker and Tessmar-Raible 2020). Indeed, for all living organisms, an internal tracking

306 of time offers major advantages compared with solely being able to directly respond to  
307 environmental changes (Helm *et al.* 2017). Intrinsicly, organisms benefit from endogenous  
308 clock(s) by maintaining a temporal organization of different cellular and physiological  
309 processes so that they occur, or not, at the same time. Relatively to their environment,  
310 organisms benefit from internal clocks for anticipation of periodic environmental changes  
311 (e.g. light availability, temperature...) and synchronization of physiological processes  
312 accordingly. Ecologically, internal clocks are crucial for synchronizing biological processes at  
313 the population level (e.g. population synchronization of external spawning events, such as  
314 observed in oysters (Bernard *et al.* 2016)), as well as the inter-specific interactions level (e.g.  
315 the diel vertical migration of zooplankton, that would be a trade-off between predator  
316 avoidance and food supply (Last *et al.* 2016)). Finally, the biochemistry of a biotope is shaped  
317 by the temporal organization of biological processes such as respiration, feeding and excretion  
318 of organisms leaving there (Helm *et al.* 2017).

319 The influence of the extreme Arctic light regime on bivalves species has already been  
320 observed at the annual scale (Ballesta-Artero *et al.* 2017; Tran *et al.* 2020b). A previous study  
321 on *Mytilus sp.* in the high Arctic showed annual rhythms of its valve behavior and shell  
322 growth, with a positive correlation of both parameters with photoperiod (Tran *et al.* 2020b).  
323 The same pattern is observed in our study, with a maximum valve opening amplitude during  
324 polar day. Furthermore, our results go further by showing that the annual trajectory of the sun  
325 continues to shape mussels valve behavior during polar day, with a positive correlation  
326 between valve amplitude and sun elevation angle above the horizon, while no significant  
327 effect of water temperature has been observed.

328 Daily rhythms in bivalve species have been described in temperate species, including *Mytilus*  
329 *sp.*, in both field studies and lab experiments, associated with a functional endogenous  
330 circadian clock machinery (Ameyaw-Akumfi and Naylor 1987; García-March *et al.* 2008;  
331 Mat *et al.* 2012; Payton *et al.* 2017b; Comeau *et al.* 2018; Chapman *et al.* 2020). A recent  
332 study has shown the persistence of *Mytilus sp.* daily behavioral rhythms during the high  
333 Arctic polar night, synchronized by both lunar day moonlight oscillations, and daily sunlight  
334 oscillations below the horizon (Tran *et al.* 2023). Here, we show for the first time the  
335 persistence of daily behavioral rhythm during polar day in a benthic species, *Mytilus sp.*, with  
336 a maximum valve amplitude around midday, despite the fact that the sun is always above the  
337 horizon, but corresponding to the higher light intensity during the day. These results reinforce  
338 previous finding of persistent daily rhythms during Arctic polar day in terrestrial vertebrates  
339 and insects (Krüll 1976; Nordtug and Mela 1988; Stelzer and Chittka 2010; Williams *et al.*

340 2015; Arnold *et al.* 2018). Similar observations have been made in pelagic zooplankton  
341 species, coinciding with persistent oscillations of the circadian clock gene expression in the  
342 copepod *Calanus finmarchicus* (Dale and Kaartvedt 2000; Fortier *et al.* 2001; Hüppe *et al.*  
343 2020; Payton *et al.* 2021). A functional clockwork has also been associated with a persistent  
344 rhythmic behavior in the Arctic scallop *Chlamys islandica* during polar night, when the sun is  
345 always below the horizon (Tran *et al.* 2016; Perrigault *et al.* 2020). Our results suggest that the  
346 circadian clock would stay functional in bivalves such as *Mytilus sp.* during the Arctic polar  
347 day, although a direct response to light cannot be excluded. Indeed, despite a weak  
348 synchronization, illustrated by individual daily periods not exactly at 24 h but rather between  
349 20 and 25 h, the common pattern at the group level with a maximal VOA around midday  
350 highly suggest that mussels are still able to detect and track sun diel changes during polar day.  
351 At least two hypotheses could be suggested. First, *Mytilus sp.* would be able to be  
352 synchronized by very weak changes of high sun intensity caused by low diel variations of sun  
353 angle in the sky constantly above the horizon. Secondly, *Mytilus sp.* would be able to be  
354 synchronized by subtle diel changes in light spectral composition. Indeed, even if the sun is  
355 always above the horizon, the light spectrum is redshifted when the sun is closer to the  
356 horizon, around midnight, while around midday, light spectrum is blueshifted (Nordtug and  
357 Mela 1988). Interestingly, while diel changes of spectral composition are presumably less  
358 intense in the middle of polar day, when the sun is permanently far away from the horizon, no  
359 clear changes of daily rhythms prevalence occur along polar day. These two hypotheses  
360 suggest that *Mytilus sp.* possesses very sensitive molecular light sensors in its tissues, able to  
361 detect weak changes in light intensity and/or quality, even at high intensity of sun  
362 illumination. These results highlight the need to investigate opsins and cryptochrome families  
363 in bivalves species, proteins known to be involved in light reception and clock  
364 synchronization, as well as to characterize physically diel light changes in intensity and  
365 quality during polar day in the Arctic (Oliveri *et al.* 2014).

366 Besides the daily rhythm, we show in our study that other cycles, related to the moon, also  
367 shape mussels' behavior in the high Arctic polar day. A very clear tidal rhythm exists but is  
368 less commonly expressed than the daily one, probably due to the low tidal amplitude at the  
369 study site (< 1 m during polar day). The plasticity between tidal and daily rhythms, with a  
370 balance between one or the other relevant to each location, have already been described in  
371 bivalve and crustacean species (Enright 1976; García-March *et al.* 2008; Tran *et al.* 2020a;  
372 Hüppe *et al.* 2020; Payton *et al.* 2021). Additionally, as already shown in other bivalve species  
373 in temperate areas, mussels also exhibit a semi-lunar rhythm, known to be entrained by neap-



374 spring tidal cycles that modulates the amplitude of the tidal cycle (García-March *et al.* 2008;  
375 Tran *et al.* 2011; Payton *et al.* 2017a; Payton and Tran 2019). Finally, we show that mussels  
376 exhibit a lunar rhythm of valve behavior. That result corroborates the recent study showing  
377 that *Mytilus sp.* expresses lunar behavioral rhythm at the same location during polar night  
378 (Tran *et al.* 2023). However, if the moonlight entrainment during polar night is intuitively  
379 clear, how the mussels are entrained by the lunar cycle in a context of permanent illumination  
380 is an open question. This finding could be a strong argument to argue that *Mytilus sp.*  
381 possesses an endogenous lunar clock that maintains a strong circalunar rhythm, even in  
382 absence of moonlight entrainment, during polar day. Another suggestion would be that other  
383 cues than lunar illumination, such as magnetic field, tidal vibrations could synchronize  
384 animals with the lunar cycle (Andreatta and Tessmar-Raible 2020). For example, the beat  
385 hypothesis developed by Erwin Bünning says that a combination of the circadian clock and  
386 the circatidal/circalunidian clock would be able to produce a circa(semi)lunar rhythm (Kaiser  
387 and Neumann). Both hypotheses highlight the need to decipher the complexity of lunar  
388 rhythms.

389 All in all, the eyeless bivalve and reemerging polar resident *Mytilus sp.* appears to exhibit  
390 multitude behavioral rhythm periodicities despite the extreme photic conditions of Arctic polar  
391 day. Interestingly, these valve behavior rhythms are observable despite the overall high valve  
392 amplitude opening of mussels during Arctic polar day. Thus, the difference in mean VOA for  
393 defined phases of daily, tidal, semilunar and lunar rhythms is narrow, suggesting that small  
394 changes of VOA may have a biological implication. Marine bivalves are an essential component  
395 of the benthic community. As filter-feeders, they feed on phytoplankton and bacterial  
396 communities. The valve behavior rhythms observed in our study are highly probably related to  
397 nutrition and respiration rhythms. The multitude of periodicities, synchronized to both sun and  
398 moon-related cycles, may confer internal and/or external advantages for mussels, in terms of  
399 activity, feeding, predation or UV protection, that remain to be understood. By cascading  
400 effects, mussels' biological rhythms may shape species communities and biogeochemical  
401 cycles in their close environment, with consequences on the Arctic ecosystems functioning. As  
402 a matter of fact, *Mytilus sp.* appears as a very tolerant and adaptive species. Its ability to deal  
403 with drastic light regimes may confer internal and external advantages, explaining their  
404 northward shift in distribution and new resettlement in high Arctic.

405

406 **Supplementary Information** The online version contains supplementary material available at

407 xxxxxxxxxxxxxxxxxxxxxxxxx

408 **Acknowledgements** We thank C. Portier, M. Sow, J. Berge, P.E. Renaud, G. Tran and S.  
409 Duveau for technical assistance and discussion. Authors also thank the AWI center for  
410 scientific diving for their help to biosensors deployment. We thank the reviewers.

411 **Author contributions** Study design and methodology: D.T., L.P., P.C., H.A., C.B., L.C.;  
412 biosensor manufacture: P.C., D.T.; fieldwork: D.T., P.C., H.A., C.B.; data treatment: A.L.M.,  
413 L.P., D.T.; interpretation: A.L.M., L.P., D.T.; manuscript writing: A.L.M., L.P., D.T.; review  
414 and editing: all authors; funding: D.T., L.C., H.A. All authors contributed critically to the drafts,  
415 and gave final approval for publication.

416 **Funding** This work was supported by the French National Research Agency (ANR),  
417 WAQMOS project 15-CE04-0002 (2015-2020), the French Polar Institute, IPEV  
418 (ARCTICLOCK project 1166), the Svalbard Environmental Protection Fund (project 15/133)  
419 and the High North Research Centre for Climate and the Environment (Fram Centre)  
420 throughout the flagship "Effects of climate change on sea and coastal ecology in the north".

421 **Data availability** All data generated or analyzed during this study are included in this published  
422 article and its supplementary information files.

423

## 424 **Declarations**

425

426 **Conflict of interest** We have no competing interests.

427 **Ethical approval** All experiments complied with the laws in effect in Svalbard and they  
428 conformed to international ethical standards.

429 **References**

- 430 Abhilash L, Shindey R, Sharma VK (2017) To be or not to be rhythmic? A review of studies  
431 on organisms inhabiting constant environments. *Biol Rhythm Res* 48:677–691. doi:  
432 10.1080/09291016.2017.1345426
- 433 Ameyaw-Akumfi C, Naylor E (1987) Temporal patterns of shell-gape in *Mytilus edulis*. *Mar*  
434 *Biol* 95:237–242. doi: 10.1007/BF00409011
- 435 Andrade H, Massabuau J-C, Cochrane S, Ciret P, Tran D, Sow M, Camus L (2016) High  
436 frequency non-invasive (HFNI) bio-sensors as a potential tool for marine monitoring  
437 and assessments. *Front Mar Sci*. doi: 10.3389/fmars.2016.00187
- 438 Andreatta G, Tessmar-Raible K (2020) The Still Dark Side of the Moon: Molecular  
439 Mechanisms of Lunar-Controlled Rhythms and Clocks. *J Mol Biol* 432:3525–3546.  
440 doi: 10.1016/j.jmb.2020.03.009
- 441 Arnold W, Ruf T, Loe LE, Irvine RJ, Ropstad E, Veiberg V, Albon SD (2018) Circadian  
442 rhythmicity persists through the Polar night and midnight sun in Svalbard reindeer. *Sci*  
443 *Rep* 8:14466. doi: 10.1038/s41598-018-32778-4
- 444 Ballesta-Artero I, Witbaard R, Carroll ML, van der Meer J (2017) Environmental factors  
445 regulating gaping activity of the bivalve *Arctica islandica* in Northern Norway. *Mar*  
446 *Biol* 164:116. doi: 10.1007/s00227-017-3144-7
- 447 Beaugrand G, Conversi A, Atkinson A, Cloern J, Chiba S, Fonda-Umani S, Kirby RR, Greene  
448 CH, Goberville E, Otto SA, Reid PC, Stemmann L, Edwards M (2019) Prediction of  
449 unprecedented biological shifts in the global ocean. *Nat Clim Change* 9:237–243. doi:  
450 10.1038/s41558-019-0420-1
- 451 Berge J, Johnsen G, Nilsen F, Gulliksen B, Slagstad D (2005) Ocean temperature oscillations  
452 enable reappearance of blue mussels *Mytilus edulis* in Svalbard after a 1000 year  
453 absence. *Mar Ecol Prog Ser* 303:167–175. doi: 10.3354/meps303167
- 454 Bernard I, Massabuau J-C, Ciret P, Sow M, Sottolichio A, Pouvreau S, Tran D (2016) In situ  
455 spawning in a marine broadcast spawner, the Pacific oyster *Crassostrea gigas*: Timing  
456 and environmental triggers. *Limnol Oceanogr* 61:635–647. doi: 10.1002/lno.10240
- 457 Bertolini E, Schubert FK, Zanini D, Sehadová H, Helfrich-Förster C, Menegazzi P (2019)  
458 Life at High Latitudes Does Not Require Circadian Behavioral Rhythmicity under  
459 Constant Darkness. *Curr Biol*. doi: 10.1016/j.cub.2019.09.032
- 460 Bingham C, Arbogast B, Guillaume GC, Lee JK, Halberg F (1982) Inferential statistical  
461 methods for estimating and comparing cosinor parameters. *Chronobiologia* 9:397–  
462 439.
- 463 Bloch G, Barnes BM, Gerkema MP, Helm B (2013) Animal activity around the clock with no  
464 overt circadian rhythms: patterns, mechanisms and adaptive value. *Proc Biol Sci*  
465 280:20130019. doi: 10.1098/rspb.2013.0019
- 466 Box GEP, Jenkins GM, Reinsel GC, Ljung GM (2015) Time series analysis: Forecasting and  
467 control. John Wiley & Sons

- 468 Chapman EC, O'Dell AR, Meligi NM, Parsons DR, Rotchell JM (2017) Seasonal expression  
469 patterns of clock-associated genes in the blue mussel *Mytilus edulis*. *Chronobiol Int*  
470 34:1300–1314. doi: 10.1080/07420528.2017.1363224
- 471 Chapman EC, Bonsor BJ, Parsons DR, Rotchell JM (2020) Influence of light and temperature  
472 cycles on the expression of circadian clock genes in the mussel *Mytilus edulis*. *Mar*  
473 *Environ Res* 159:104960. doi: 10.1016/j.marenvres.2020.104960
- 474 Chylek P, Folland C, Klett JD, Wang M, Hengartner N, Lesins G, Dubey MK (2022) Annual  
475 Mean Arctic Amplification 1970–2020: Observed and Simulated by CMIP6 Climate  
476 Models. *Geophys Res Lett* 49:e2022GL099371. doi: 10.1029/2022GL099371
- 477 Comeau LA, Babarro JMF, Longa A, Padin XA (2018) Valve-gaping behavior of raft-  
478 cultivated mussels in the Ría de Arousa, Spain. *Aquac Rep* 9:68–73. doi:  
479 10.1016/j.aqrep.2017.12.005
- 480 Dale T, Kaartvedt S (2000) Diel patterns in stage-specific vertical migration of *Calanus*  
481 *finmarchicus* in habitats with midnight sun. *ICES J Mar Sci* 57:1800–1818. doi:  
482 10.1006/jmsc.2000.0961
- 483 Enright JT (1976) Plasticity in an isopod's clockworks: Shaking shapes form and affects  
484 phase and frequency. *J Comp Physiol* 107:13–37. doi: 10.1007/BF00663916
- 485 Fortier M, Fortier L, Hattori H, Saito H, Legendre L (2001) Visual predators and the diel  
486 vertical migration of copepods under Arctic sea ice during the midnight sun. *J*  
487 *Plankton Res* 23:1263–1278. doi: 10.1093/plankt/23.11.1263
- 488 García-March JR, Sanchís Solsona MÁ, García-Carrascosa AM (2008) Shell gaping  
489 behaviour of *Pinna nobilis* L., 1758: circadian and circalunar rhythms revealed by in  
490 situ monitoring. *Mar Biol* 153:689–698. doi: 10.1007/s00227-007-0842-6
- 491 Gouthiere L, Mauvieux B, Davenne D, Waterhouse J (2005) Complementary methodology in  
492 the analysis of rhythmic data, using examples from a complex situation, the  
493 rhythmicity of temperature in night shift workers. *Biol Rhythm Res* 36:177–193. doi:  
494 10.1080/09291010400026298
- 495 Häfker NS, Tessmar-Raible K (2020) Rhythms of behavior: are the times changin'? *Curr*  
496 *Opin Neurobiol* 60:55–66. doi: 10.1016/j.conb.2019.10.005
- 497 Helm B, Visser ME, Schwartz W, Kronfeld-Schor N, Gerkema M, Piersma T, Bloch G (2017)  
498 Two sides of a coin: ecological and chronobiological perspectives of timing in the  
499 wild. *Philos Trans R Soc B Biol Sci* 372:20160246. doi: 10.1098/rstb.2016.0246
- 500 Huffeldt NP (2020) Photic Barriers to Poleward Range-shifts. *Trends Ecol Evol*. doi:  
501 10.1016/j.tree.2020.04.011
- 502 Hüppe L, Payton L, Last K, Wilcockson D, Ershova E, Meyer B (2020) Evidence for  
503 oscillating circadian clock genes in the copepod *Calanus finmarchicus* during the  
504 summer solstice in the high Arctic. *Biol Lett* 16:20200257. doi:  
505 10.1098/rsbl.2020.0257

- 506 Kaiser TS, Neumann J Circalunar clocks—Old experiments for a new era. *BioEssays*  
507 n/a:2100074. doi: 10.1002/bies.202100074
- 508 Krüll F (1976) Zeitgebers for animals in the continuous daylight of high arctic summer.  
509 *Oecologia* 24:149–157. doi: 10.1007/BF00572756
- 510 Last KS, Hobbs L, Berge J, Brierley AS, Cottier F (2016) Moonlight drives Ocean-scale mass  
511 vertical migration of zooplankton during the Arctic winter. *Curr Biol* 26:244–251. doi:  
512 10.1016/j.cub.2015.11.038
- 513 Leopold P, Renaud PE, Ambrose WG, Berge J (2019) High Arctic *Mytilus* spp.: occurrence,  
514 distribution and history of dispersal. *Polar Biol* 42:237–244. doi: 10.1007/s00300-018-  
515 2415-1
- 516 Mat AM, Massabuau J-C, Ciret P, Tran D (2012) Evidence for a Plastic Dual Circadian  
517 Rhythm in the Oyster *Crassostrea gigas*. *Chronobiol Int* 29:857–867. doi:  
518 10.3109/07420528.2012.699126
- 519 Mathiesen SS, Thyrring J, Hemmer-Hansen J, Berge J, Sukhotin A, Leopold P, Bekaert M,  
520 Sejr MK, Nielsen EE (2017) Genetic diversity and connectivity within *Mytilus* spp. in  
521 the subarctic and Arctic. *Evol Appl* 10:39–55. doi: 10.1111/eva.12415
- 522 Mermet J, Yeung J, Naef F (2017) Systems Chronobiology: Global Analysis of Gene  
523 Regulation in a 24-Hour Periodic World. *Cold Spring Harb Perspect Biol* 9:a028720.  
524 doi: 10.1101/cshperspect.a028720
- 525 Nelson W, Tong YL, Lee JK, Halberg F (1979) Methods for cosinor-rhythmometry.
- 526 Nordtug T, Mela TB (1988) Diurnal variations in natural light conditions at summer time in  
527 arctic and subarctic areas in relation to light detection in insects. *Ecography* 11:202–  
528 209. doi: 10.1111/j.1600-0587.1988.tb00802.x
- 529 Oliveri P, Fortunato AE, Petrone L, Ishikawa-Fujiwara T, Kobayashi Y, Todo T, Antonova O,  
530 Arboleda E, Zantke J, Tessmar-Raible K, Falciatore A (2014) The  
531 cryptochrome/photolyase family in aquatic organisms. *Mar Genomics* 14:23–37. doi:  
532 10.1016/j.margen.2014.02.001
- 533 Payton L, Tran D (2019) Moonlight cycles synchronize oyster behaviour. *Biol Lett*  
534 15:20180299. doi: 10.1098/rsbl.2018.0299
- 535 Payton L, Sow M, Massabuau J-C, Ciret P, Tran D (2017a) How annual course of  
536 photoperiod shapes seasonal behavior of diploid and triploid oysters, *Crassostrea*  
537 *gigas*. *PLOS ONE* 12:e0185918. doi: 10.1371/journal.pone.0185918
- 538 Payton L, Perrigault M, Hoede C, Massabuau J-C, Sow M, Huvet A, Boullot F, Fabioux C,  
539 Hegaret H, Tran D (2017b) Remodeling of the cycling transcriptome of the oyster  
540 *Crassostrea gigas* by the harmful algae *Alexandrium minutum*. *Sci Rep* 7:3480. doi:  
541 10.1038/s41598-017-03797-4
- 542 Payton L, Hüppe L, Noirot C, Hoede C, Last KS, Wilcockson D, Ershova E, Valière S, Meyer  
543 B (2021) Widely rhythmic transcriptome in *Calanus finmarchicus* during the high  
544 Arctic summer solstice period. *iScience*. doi: 10.1016/j.isci.2020.101927

- 545 Perrigault M, Andrade H, Bellec L, Ballantine C, Camus L, Tran D (2020) Rhythms during  
546 the polar night: evidence of clock-gene oscillations in the Arctic scallop *Chlamys*  
547 *islandica*. *Proc R Soc B Biol Sci* 287:20201001. doi: 10.1098/rspb.2020.1001
- 548 Post E, Steinman BA, Mann ME (2018) Acceleration of phenological advance and warming  
549 with latitude over the past century. *Sci Rep* 8:3927. doi: 10.1038/s41598-018-22258-0
- 550 R Core Team (2013) R: The R project for statistical computing. <https://www.r-project.org/>.
- 551 Scargle JD (1982) Studies in astronomical time series analysis. II-Statistical aspects of  
552 spectral analysis of unevenly spaced data. *Astrophys J* 263:835–853.
- 553 Schmal C, Herzel H, Myung J (2020) Clocks in the Wild: Entrainment to Natural Light. *Front*  
554 *Physiol*. doi: 10.3389/fphys.2020.00272
- 555 Stelzer RJ, Chittka L (2010) Bumblebee foraging rhythms under the midnight sun measured  
556 with radiofrequency identification. *BMC Biol* 8:93. doi: 10.1186/1741-7007-8-93
- 557 Tessmar- Raible K, Raible F, Arboleda E (2011) Another place, another timer: Marine  
558 species and the rhythms of life. *BioEssays* 33:165–172. doi: 10.1002/bies.201000096
- 559 Tran D, Ciret P, Ciutat A, Durrieu G, Massabuau J-C (2003) Estimation of potential and  
560 limits of bivalve closure response to detect contaminants: Application to cadmium.  
561 *Environ Toxicol Chem* 22:914–920. doi: 10.1002/etc.5620220432
- 562 Tran D, Nadau A, Durrieu G, Ciret P, Parisot J-P, Massabuau J-C (2011) Field chronobiology  
563 of a molluscan bivalve: How the Moon and Sun cycles interact to drive oyster activity  
564 rhythms. *Chronobiol Int* 28:307–317. doi: 10.3109/07420528.2011.565897
- 565 Tran D, Sow M, Camus L, Ciret P, Berge J, Massabuau J-C (2016) In the darkness of the  
566 polar night, scallops keep on a steady rhythm. *Sci Rep* 6:1–9. doi: 10.1038/srep32435
- 567 Tran D, Perrigault M, Ciret P, Payton L (2020a) Bivalve mollusc circadian clock genes can  
568 run at tidal frequency. *Proc R Soc B Biol Sci* 287:20192440. doi:  
569 10.1098/rspb.2019.2440
- 570 Tran D, Andrade H, Durier G, Ciret P, Leopold P, Sow M, Ballantine C, Camus L, Berge J,  
571 Perrigault M (2020b) Growth and behaviour of blue mussels, a re-emerging polar  
572 resident, follow a strong annual rhythm shaped by the extreme high Arctic light  
573 regime. *R Soc Open Sci* 7:200889. doi: 10.1098/rsos.200889
- 574 Tran D, Andrade H, Camus L, Leopold P, Ballantine C, Berge J, Durier G, Sow M, Ciret P  
575 (2023) Evidence of separate influence of moon and sun on light synchronization of  
576 mussel's daily rhythm during the polar night. *iScience*. doi:  
577 10.1016/j.isci.2023.106168
- 578 Vihtakari M (2022) ggOceanMaps: Plot Data on Oceanographic Maps using “ggplot2”. R  
579 package version 1.2.6, <https://mikkovihtakari.github.io/ggOceanMaps/>.
- 580 Williams CT, Barnes BM, Buck CL (2015) Persistence, Entrainment, and Function of  
581 Circadian Rhythms in Polar Vertebrates. *Physiology* 30:86–96. doi:  
582 10.1152/physiol.00045.2014

583 (2021) Arctic assessment report shows faster rate of warming.  
584 [https://public.wmo.int/en/media/news/arctic-assessment-report-shows-faster-rate-of-](https://public.wmo.int/en/media/news/arctic-assessment-report-shows-faster-rate-of-warming)  
585 [warming](https://public.wmo.int/en/media/news/arctic-assessment-report-shows-faster-rate-of-warming). Accessed 14 Jul 2022

586